ACS OMEGA

Article

Cite This: ACS Omega 2018, 3, 7432−7440

Structural Motif Descriptors as a Way To Elucidate the Agonistic or Antagonistic Activity of Growth Hormone−Releasing Hormone Peptide Analogues

Kevin Jeanne Dit Fouque,[†] Luis M. Salgueiro,[‡,§] Renzhi Cai,[‡,§] Wei Sha,[‡,§] Andrew V. Schally,[‡,§] and Francisco Fernandez-Lima*[,†,∥]

[†]Department of Chemistry and Biochemistry, Florida International University, 11200 SW 8th Street, AHC4-233, Miami, Florida 33199, United States

[‡]Veterans Affairs Medical Center, 1201 NW 16th Street, Research Service (151), Room 2A103C, Miami, Florida 33125, United States

[§]Departments of Pathology and Medicine, Divisions of Hematology/Oncology and Endocrinology, Miller School of Medicine, University of Miami, 1600 NW 10th Avenue #1140, Miami, Florida 33136, United States

[∥]Biomolecular Sciences Institute, Florida International University, 11200 SW 8th Street, AHC4-211, Miami, Florida 33199, United States

Supporting Information

ABSTRACT: The synthesis of analogues of hypothalamic neuropeptide growth hormone−releasing hormone (GHRH) is an efficient strategy for designing new therapeutic agents. Several promising synthetic agonist and antagonist analogues of GHRH have been developed based on amino acid mutations of the GHRH (1−29) sequence. Because structural information on the activity of the GHRH agonists or antagonists is limited, there is a need for more effective analytical workflows capable of correlating the peptide sequence with biological activity. In the present work, three GHRH agonists—MR-356, MR-406, and MR-409—and three GHRH antagonists—MIA-602, MIA-606, and MIA-690—were investigated to assess the role of substitutions in the amino acid sequence on structural motifs and receptor binding affinities. The use of high resolution trapped ion mobility spectrometry coupled to mass spectrometry allowed the observation of a large number of peptide-specific mobility bands (or structural motif descriptors) as a function of the amino acid sequence and the starting solution environment. A direct correlation was observed between the amino acid substitutions (i.e., basic residues and D/L-amino acids), the structural motif descriptors, and the biological function (i.e., receptor binding affinities of the GHRH agonists and antagonists). The simplicity, ease, and high throughput of the proposed workflow based on the structural motif descriptors can significantly reduce the cost and time during screening of new synthetic peptide analogues.

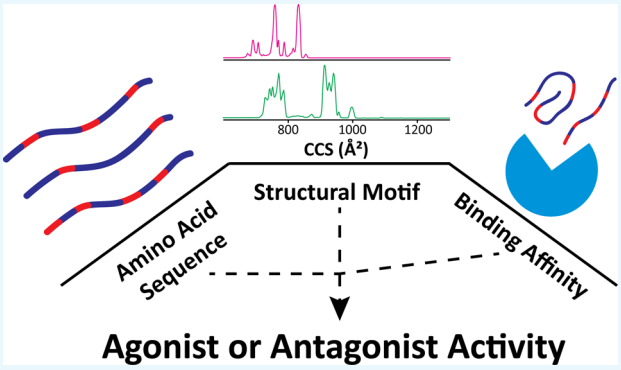

1. INTRODUCTION

Growth hormone−releasing hormone (GHRH) is a hypothalamic peptide hormone containing 44 residues that stimulate the secretion and release of growth hormone (GH) from the anterior pituitary gland upon binding to its receptor (GHRH-R).[1] Since the characterization of the sequence of GHRH (Figure S1a), this hypothalamic neuropeptide has been the focus of intense studies.[2,3] Biological tests of GHRH revealed that the structural requirements for growth hormone−stimulating activity resided in the N-terminal 1−29 residues of this peptide (Figure S1b).[4] The GHRH peptide and GHRH-R are also expressed in various normal human tissues, including breast, colon, esophagus, kidney, liver, lung, ovary, pancreas, prostate, testis, and thymus,[5−7] and in many human cancer cell lines and tumors.[1,8−11] A major drawback in using native GHRH as a therapeutic agent is its short in vivo half-life due to degradation by proteolytic enzymes.[12] Understanding the action of GHRH on its target cells is important for the development of various degradation-resistant synthetic GHRH analogues, which may provide a promising approach for drug design. Previous reports have shown the advantages of the synthesis of GHRH antagonists to develop therapies for the management of diverse cancers and other diseases.[1,8,13] It has been demonstrated that the inhibitory effects of the

Received: March 1, 2018
Accepted: June 21, 2018
Published: July 6, 2018

DOI: 10.1021/acsomega.8b00375
ACS Omega 2018, 3, 7432−7440

GHRH antagonists on the growth of various tumors are exerted in part by an indirect endocrine mechanism through the suppression of GHRH-evoked release of GH from the pituitary, resulting in the decrease in the production of hepatic insulin-like growth factor I.[1,8] Direct mechanisms involved in the main antitumor effects of GHRH antagonists appear to be based on blocking the action of autocrine GHRH on tumors.[1,8] It has been also demonstrated that the GHRH antagonists inhibit the growth of androgen-dependent and -independent human prostatic cancers and diverse human tumors xenografted into nude mice, and reduce the tumoral growth factors.[1,14−17] In addition, the development of GHRH agonists with a prolonged half-life has been achieved.[18] Synthetic GHRH agonists have been shown to exert direct effects on various extra-pituitary cells/tissues.[18] Recent studies have exhibited that these analogues improve the survival and proliferation of pancreatic β-islet cells, providing evidence of a promising pharmacological therapy in diabetic patients.[19,20] GHRH agonists also showed a cardioprotective effect in activating myocardial repair after a heart attack, and promote the survival of cardiac stem cells.[21,22] Other findings exhibited that agonistic GHRH may have clinical use in improving the healing of skin wounds resulting from trauma and/or disease.[23]

The accumulating results of these studies demonstrate the importance of further synthesis of GHRH agonists and antagonists because of their likely multiple therapeutic roles in a wide range of medical fields. However, it is worth mentioning that to date, although the biological activity of these analogues has been demonstrated, a direct correlation between the amino acid sequence and their agonist/antagonist potency has not been determined. The structural characterization of GHRH agonists and antagonists, and the understanding of the structural motifs responsible for a given agonist/antagonist function remain to be understood. Recent efforts based on in silico directed evolution have attempted to link the amino acid sequence with the biological activity as a way to develop leading mutants.[24,25] However, the main limitation of the current in silico directed evolution algorithms is the lack of experimental descriptors per amino acid sequence. Gas phase, post-ionization tools based on soft ionization techniques (e.g., electrospray source ionization (ESI)[26]) coupled to ion mobility spectrometry-mass spectrometry (IMS-MS), which are different from NMR- and X-ray crystallography-based structural biology studies, have shown unique advantages in the description of peptide kinetic intermediates under native and denaturing solution conditions.[27−30]

In the present study, we took advantage of a recently developed, but previously untested, high-resolution trapped IMS-MS technology (TIMS-MS)[31−34] to generate a high-throughput screening workflow capable of correlating the primary and secondary structures of the GHRH analogues and their receptor-binding affinity using descriptors of the GHRH conformational space and response to the molecular environment. The advantage of the ESI evaporative cooling of the solvent, leading to a freezing of multiple stable conformations, known as the memory effect,[35,36] was used to determine the correlation between the TIMS-MS structural descriptors of the GHRH analogues and variations on the starting solution environment. A statistical model is described to correlate the effects of the substitutions in the amino acid sequence on the number of structural motifs and receptor binding affinities. The performance of the workflow was successfully evaluated using a set of three GHRH agonists—MR-356, MR-406, and MR-409—and three GHRH antagonists—MIA-602, MIA-606, and MIA-690 (Table 1 and Figure S1b).

2. RESULTS AND DISCUSSION

2.1. Structural Motif Sampling of GHRH Agonists and Antagonists. The possibility to study kinetically trapped intermediates of biomolecules using TIMS-MS enables the characterization of multiple structural motifs in a single experiment and their dependence on the molecular environment.[37−39] For example, solvent conditions can induce conformational changes, and these changes are reflected in the number of mobility bands and the distribution of the charge state.[40,41] In the case of GHRH, the charge state distribution and the structural motif analysis of the GHRH agonists—MR-356, MR-406, and MR-409—and antagonists—MIA-602, MIA-606, and MIA-690—showed a direct dependence on the molecular environment (i.e., starting solvent condition) (Figure 1). Differences in the distribution of the charge state with the molecular environment derive from differences in the amino acid sequence (i.e., number of basic residues) of the GHRH analogues due to different proton affinities. For example, the GHRH agonists have 5 basic residues (positions 11, 12, 20, 21, and 29), whereas the GHRH antagonists have 8 or 9 basic residues (positions 2, 9, 11, 12, 20, 21, 28, 29, and 30). As a general trend, an increase in the higher charge states is observed, when the solvent conditions change from native to denaturing conditions, due to the exposure of the basic residues. For example, under native conditions (pH 6.7, 10 mM NH_4Ac), $[M + 3H]^{3+}$ and $[M + 4H]^{4+}$ species represent the most abundant charge states observed for the GHRH agonists and antagonists, respectively (Figure 1, left panel). An increase in the concentration of the organic content (e.g., 0−50% MeOH) showed a shift toward higher charge states (Figure 1, left panel). The impact of the starting solvent conditions on the relative abundance of the different structural motifs is better addressed in the IMS distribution of the conformational space (Figure 1, right panel). For example, major changes in the number and relative abundances of the IMS bands are observed for the GHRH analogues during native (10 mM NH_4Ac) and denaturing (50% MeOH) conditions (Figure 1, right panel). A closer inspection of the structural motifs dependence with the solvent conditions showed that an increase in abundance of the larger collision cross section (CCS, Å^2) values (more extended conformations) is observed in the denaturing conditions as compared to the native conditions (Figure 1, right panel).

The structural motif space per amino acid sequence can be further sampled by collision-induced activation (CIA) before the TIMS-MS analysis (Figure S2). Thus, the energy from the collisions can allow to overcome the conformational barriers and sample other local free energy minima not amenable by changes in the molecular environment by varying the solvent conditions.[42,43] Although ions were activated to the highest condition accessible by the current setup, no major changes in the structural motif space of the agonists and antagonists of GHRH (1−29) are observed upon CIA (i.e., same number of IMS bands and relative abundance, Figure S2). We interpret these CIA-TIMS results as that the activation energy is probably not sufficient to induce new structural changes or interconversions in the gas phase.

2.2. TIMS-MS Tool To Elucidate the Agonistic/Antagonistic Potency of Synthetic GHRH Analogues.

DOI: 10.1021/acsomega.8b00375
ACS Omega 2018, 3, 7432−7440

Table 1. Amino Acid Sequence and Molecular Weight (Daltons) of GHRH (1−29)-NH_2 and Its Synthetic GHRH Agonists, MR-356, MR-406, and MR-409, and GHRH Antagonists, MIA-602, MIA-606, and MIA-690[a]

peptides	position of amino acid residues																												
	0		1		2		6		8		9		10		11		12		15		20		21		27		28		29		30
GHRH	H		Tyr		Ala		Phe		Asn		Ser		Tyr		Arg		Lys		Gly		Arg		Lys		Met		Ser		Arg		NH_2
MR-356	H		*N*-Me-Tyr		Ala		Phe		Gln		Ser		Tyr		Arg		Orn		Abu		Arg		Orn		Nle		Asp		Agm		
MR-406	H		*N*-Me-Tyr		Ala		Phe		Gln		Ser		Tyr		Arg		Orn		Abu		Arg		Orn		Nle		Asp		Arg		NH-Me
MR-409	H		*N*-Me-Tyr		D-Ala		Phe		Asn		Ser		Tyr		Arg		Orn		Abu		Arg		Orn		Nle		Asp		Arg		NH-Me
MIA-602	PhAc-Ada		Tyr		D-Arg		Fpa_5		Ala		Har		*N*-Me-Tyr		His		Orn		Abu		His		Orn		Nle		D-Arg		Har		NH_2
MIA-606	PhAc-Ada		Tyr		D-Arg		Fpa_5		*N*-Me-Ala		Har		*N*-Me-Tyr		His		Orn		Abu		His		Orn		Nle		D-Arg		Har		Agm
MIA-690	PhAc-Ada		Tyr		D-Arg		Cpa		Ala		Har		Fpa_5		His		Orn		Abu		His		Orn		Nle		D-Arg		Har		NH_2

[a]Noncoded amino acid residues and acyl groups used in the synthesis of the GHRH analogues are abbreviated as follows: Abu: α-aminobutyric acid; Ada: 12-aminododecanoic acid; Agm: agmatine; Cpa: parachloro-phenylalanine; Fpa_5: pentafluoro-phenylalanine; Har: homoarginine; Nle: norleucine; Orn: ornithine; PhAc: phenylacetyl.

The conformational space analysis using nano-ESI-TIMS-MS resulted in multiple structural motifs (i.e., IMS bands) for every charge state of the agonists (Figure S3) and antagonists (Figure S4) of GHRH (1−29) in the native conditions. The CCS values for all the observed structural motifs of the GHRH agonists and antagonists are summarized in Tables S1 and S2, respectively. A closer inspection of the structural motif space observed for the GHRH agonists and antagonists shows a direct correlation between the mutations and the IMS profiles (Figures S3 and S4). A simplified way to assess the role of the substitutions in the amino acid sequence on the conformational space can be done by building the correlation maps of the sequences and structural motifs with a distance matrix of the receptor-binding affinities of the agonists and antagonists of GHRH (1−29) (Figures 2 and S5).

Further inspection of the correlation map based on the amino acid sequence clearly identifies two major subgroups—GHRH agonists and antagonists (Figure 2a). The clustering in two mayor groups corresponds to the relative similarity in the sequence mutation within the agonist and antagonist GHRH analogues studied. Molecular descriptors based on the IMS profiles per charge state for each amino acid sequence can provide a more detailed information on the conformational space and charge state distribution as a function of molecular environment. For example, although similar subgroups are observed when utilizing the structural motifs as descriptors during the correlation analysis of the GHRH agonists and antagonists, a more detailed information on the transcendence of a given mutation on the structural motifs and their relative abundance is observed (Figures 2b and S5). That is, significant differences in the structural motifs as a function of the substitutions in the amino acid sequence are observed, which translates into their agonist/antagonist functions. In fact, these structural motif differences are reflected in the distance matrix based on the binding affinity, clearly identifying the GHRH agonists and antagonists clusters (Figure 2c). This means that different structural motifs are probably involved in the receptor binding according to their agonist or antagonist functions. To determine which conformation is needed to bind to the receptor function as an agonist or antagonist, the three GHRH agonists—MR-356, MR-406, and MR-409—and GHRH antagonists—MIA-602, MIA-606, and MIA-690—are compared according to their structural motifs and reported receptor-binding affinities (Figure 2).

In the case of the GHRH agonists, the comparison between MR-356 and MR-406 shows that the single amino acid substitution in position 29 results in large differences in structural motifs (Figures 2 and 3a,b). MR-356 has a basic C-terminal agmatine residue, implying that the proton attachment sites are mainly localized on the three most basic residues, Arg^{11}, Arg^{20}, and Agm^{29}, mainly giving one unfolded conformation. In the case of MR-406, the Agm^{29} is modified by a less basic residue, Arg^{29}-NH-Me, implying a competition in the proton attachment site between the basic Orn^{12} and Orn^{21} residues, leading to an increase in the number of structural motifs. In addition, the replacement of Agm^{29} with Arg^{29}-NH-Me results in increasing proteolytic stability, consistent with more compact conformations. The differences in the structural motifs and their previous reported binding affinities suggest that the receptor binding is driven by the most intense compact structural motif of MR-406. This conformational space is probably responsible for the improvement in the binding affinity and therefore the agonist potency.[18]

DOI: 10.1021/acsomega.8b00375
ACS Omega 2018, 3, 7432−7440

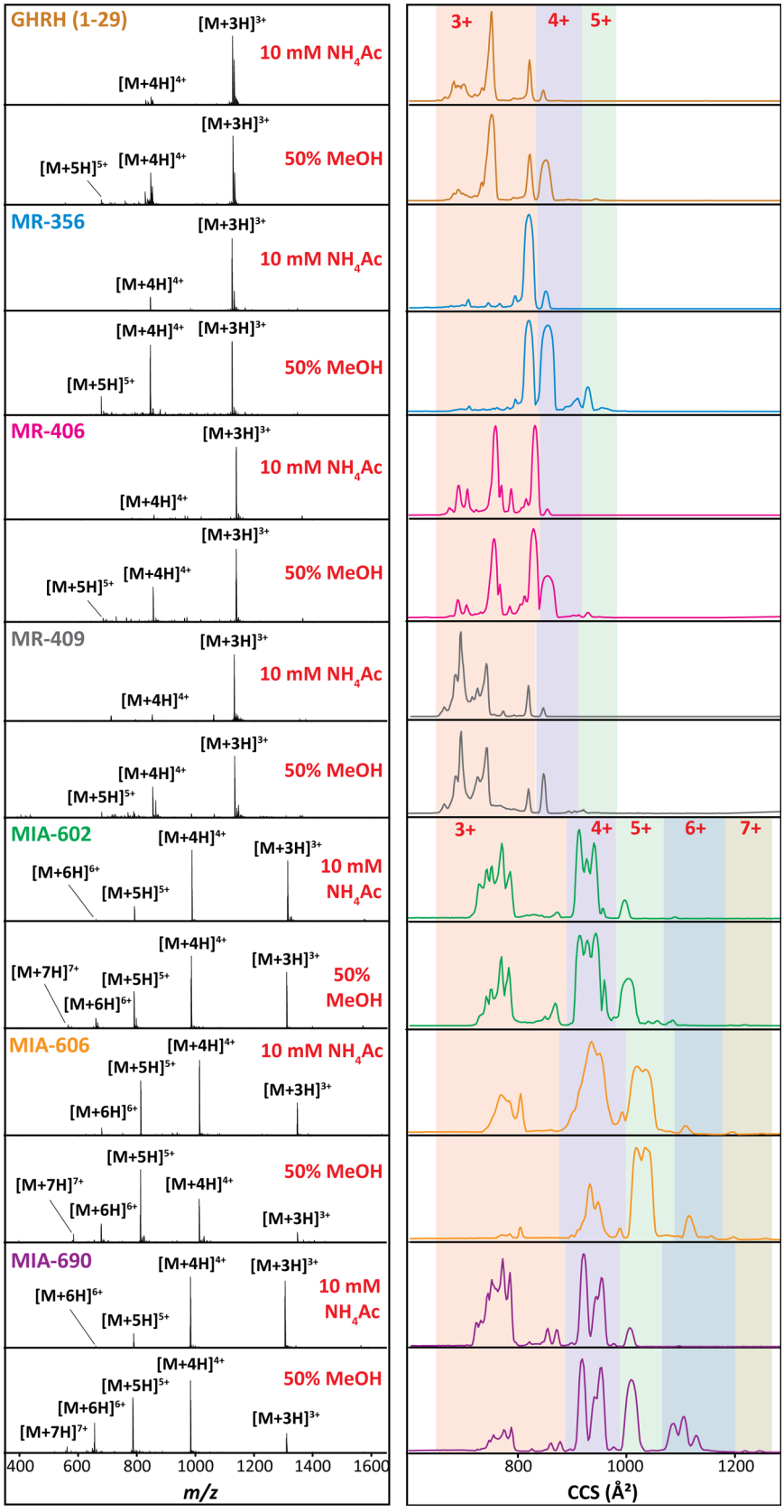

Figure 1. *Left panel*: typical mass spectra of the GHRH (1−29), agonists (MR-356, MR-406, and MR-409) and antagonists (MIA-602, MIA-606, and MIA-690) in native (10 mM NH_4Ac) and denaturing (50% MeOH) molecular environments. *Right panel*: total ion mobility profiles, obtained by summation of the IMS intensity of all the observed charge states, of GHRH (brown), MR-356 (blue), MR-406 (magenta), MR-409 (gray), MIA-602 (green), MIA-606 (orange), and MIA-690 (purple). The 3+, 4+, 5+, 6+, and 7+ charges states are highlighted using a light red, light purple, light green, light blue, and light gray background, respectively.

DOI: 10.1021/acsomega.8b00375
ACS Omega 2018, 3, 7432−7440

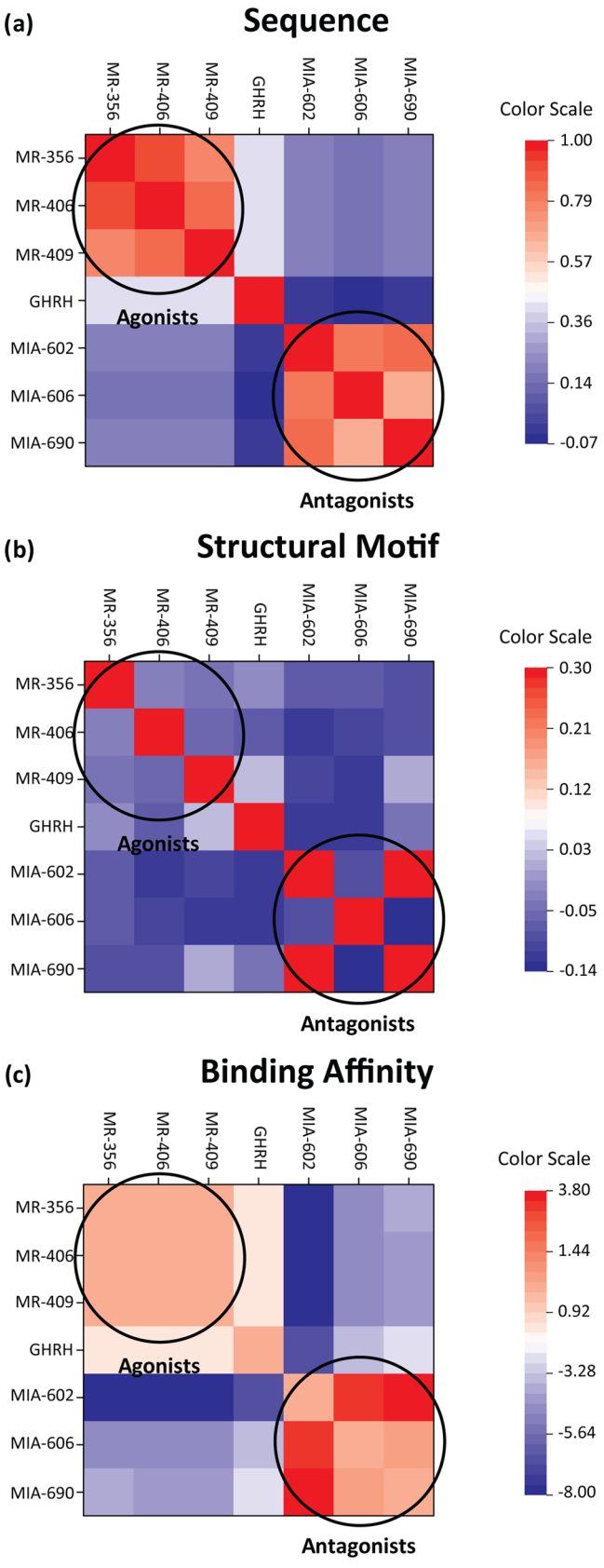

Figure 2. Correlation maps of the (a) sequence mutation and (b) structural motif and distance matrix of the (c) binding affinity of the GHRH (1−29), agonists and antagonists, in a native molecular environment. The color scale represents the similarities between the GHRH analogues going toward a strong correlation (red) to a poor correlation (blue).

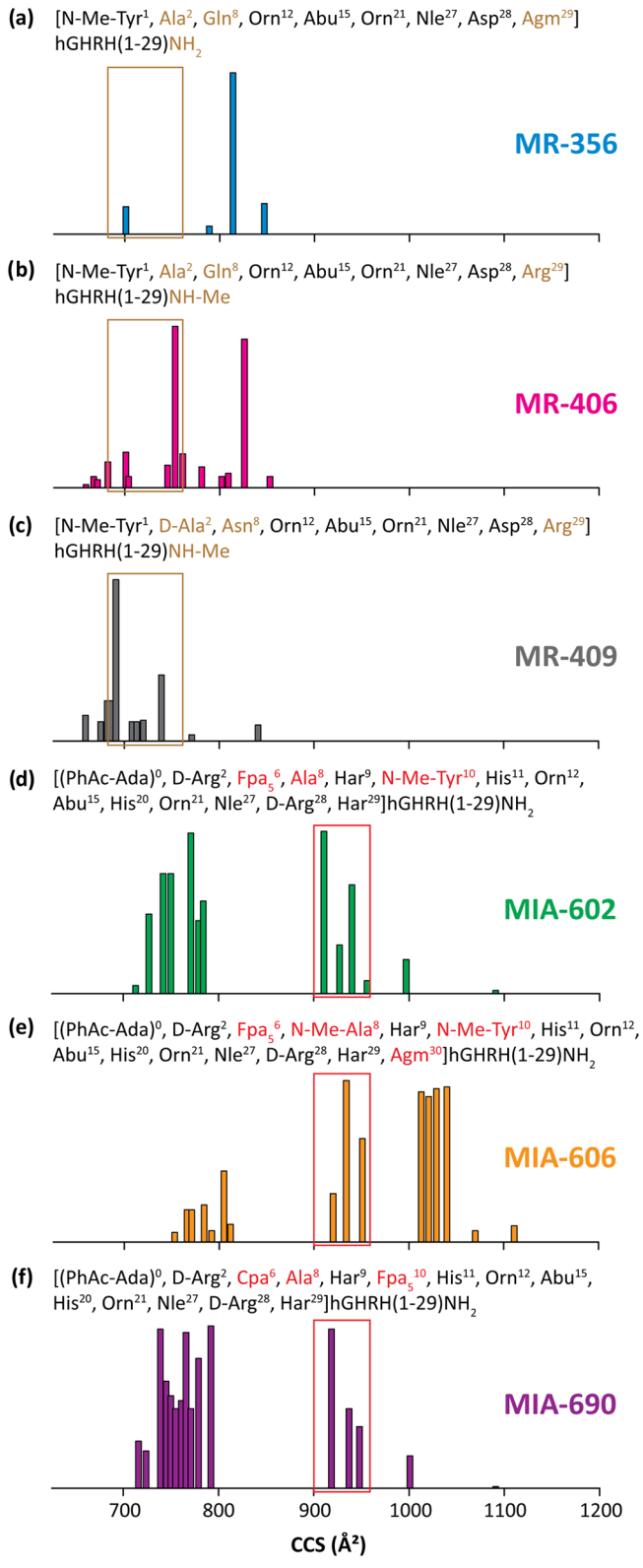

Figure 3. Discrete representations of the IMS bands for (a) MR-356 (blue), (b) MR-406 (magenta), (c) MR-409 (gray), (d) MIA-602 (green), (e) MIA-606 (orange), and (f) MIA-690 (purple) in a native molecular environment. Sequence differences are represented in brown and red for GHRH agonists and antagonists, respectively. The brown and red windows highlight the proposed structural motif region that drive the agonist and antagonist receptor binding, respectively.

DOI: 10.1021/acsomega.8b00375
ACS Omega 2018, 3, 7432−7440

The comparison between MR-406 and MR-409 indicates that the two amino acid substitutions in position 2 and 8 also result in large differences in structural motifs (Figures 2 and 3a,c). The replacement of the L-Ala^2 residue with a D-Ala^2 residue allows to improve the resistance to enzymatic degradation,[44,45] in agreement with the promotion of more compact structural motifs.[46] In contrast to the previous case, the most intense very compact conformation of MR-409 leads to a decrease in the receptor-binding affinity. In addition, our group showed that the best combination at positions 2 and 8 are D-Ala and Gln, respectively.[18] As a consequence of these observations, the structural motifs located between the most intense conformation of MR-406 and MR-409 (highlighted in brown in Figure 3a−c) probably drive the receptor binding, leading to an increase in the binding affinity, which defines the potency of the agonist function.

In the case of the GHRH antagonists, the comparison between MIA-602 and MIA-606 shows that the single amino acid substitution in position 30 results in large differences in structural motifs (Figures 2 and 3d,e). This observation suggests that the additional basic Agm^{30} residue of MIA-606 plays a major role in the structural motifs by promoting more extended structures than those observed for MIA-602. That is, the addition of a basic residue results in an increase in the intramolecular Coulombic repulsion, which, combined with the conformational flexibility of the peptide, favors more extended structural motifs. In addition, MIA-602 and MIA-606, which are known to exert a potent antagonist function,[47,48] do not share common bands in the most compact and extended structural motifs, suggesting that these conformations are probably not involved in the binding receptor (Figure 3d,e). These differences in the structural motifs, combined with their previous reported receptor-binding affinities, enable us to determine a CCS region (highlighted in red in Figure 3d−f) that probably drives the receptor binding and is therefore responsible for the increase in the antagonist potency. In addition, MIA-602 has a stronger binding affinity to the GHRH receptor than MIA-606 as previously described.[48] As a consequence, this observation can be translated in the structural motifs by the presence of a more intense extended conformation for MIA-606 in the proposed CCS region, as compared to the most intense IMS band of MIA-602 (Figure 3d,e). The insertion of the basic Agm^{30} residue in MIA-606 results in an increase in the intramolecular Coulombic repulsion in the gas phase when protonated, which typically results in a more open conformation (higher CCS). In a solution, this basic residue will have more sensitivity to the solution condition, making it less likely to behave as the original GHRH and therefore significantly changing (decreasing, in this case, the antagonist potency) the binding affinity to the GHRH receptor.[47,48]

The comparison between MIA-602 and MIA-690 displays a very strong correlation in both sequences and structural motifs, indicating that the two amino acid substitutions in positions 6 and 10 do not result in major changes in structural motifs (Figures 2 and 3d,f). This can be explained by the nature of the amino acid substitution that presents similar chemical structures (Figure S6). Despite the similarity of structural motifs, MIA-602 displays a significantly better binding affinity to the GHRH receptor than MIA-690.[47,48] As in the case of MIA-606, this could be explain by the presence of a slightly more intense extended structure for MIA-690 in the proposed CCS region, as compared to the most intense IMS band of MIA-602 (Figure 3d,f). In addition, the increase in the number and intensity of the most compact structural motifs probably plays a role in the receptor-binding affinity by competing with the conformation involved in the receptor binding. As a consequence of these observations, we propose that the structural motif region (highlighted in red in Figure 3d−f) of the GHRH antagonists probably drives the receptor binding, leading to an increase in the binding affinity, which defines the potency of the antagonist function. These results suggest that the GHRH agonists and antagonists adopt very different conformations, where compact structures are needed to bind to the receptor as an agonist function, whereas more extended conformations are required for an antagonist function.

3. CONCLUSIONS

Herein, a high-throughput workflow was developed and evaluated for the assessment of the influence of the substitutions in the amino acid sequence on the potential biological activity on the agonist/antagonist potency of GHRH analogues based on the peptides conformational space. This study showcases the power of IMS bands as potential descriptors of biological active states for the case of GHRH analogue receptor-binding affinities: agonist and antagonist. The present results reveal that the molecular environment (e.g., starting solvent conditions) and the amino acid substitution plays a significant role in the conformational space of the GHRH analogues, as reflected by the substantial changes in the number of IMS bands and their distribution. The studied correlations suggest that more compact structures are likely to present an agonist function, whereas more extended conformations are likely to have an antagonist function.

The high-throughput of the proposed screening workflow based on TIMS-MS permits the determination of characteristic structural motif descriptors of agonistic or antagonistic GHRH potencies by only requiring a minute amount of material and a short analysis time (millisecond time scale) as compared to traditional screening strategies (e.g., NMR, enzyme-linked immunosorbent assay, and Western blot) and biological activity assays. However, the latest strategies are ultimately required and complementary to the described approach because the structural motif descriptors generated by TIMS-MS correspond to the average momentum transfer CCS.

Although the basis of the correlation between primary sequence, conformational space, and biological activity was illustrated for the case of three GHRH antagonist and three agonist, further developments with larger training synthetic peptides sets can lead to better predictions of point mutations utilizing the structural motif descriptors as a fast screening step. This works provides a stepping stone toward the elucidation of the effect of the amino acid sequence on the structural motif space and receptor-binding affinity of synthetic peptides.

4. EXPERIMENTAL SECTION

4.1. Materials and Reagents. The GHRH agonists—MR-356, MR-406, and MR-409—and GHRH antagonists—MIA-602, MIA-606, and MIA-690—were synthesized by R.C. and W.S. in the laboratory of one of us (A.V.S.) using the solid-phase method and purified by reversed-phase high-performance liquid chromatography as previously reported.[18,47,49] Solutions were prepared at a final concentration of 5 μM in 10 mM ammonium acetate (NH_4Ac) for native

DOI: 10.1021/acsomega.8b00375
ACS Omega 2018, 3, 7432−7440

conditions, and in 50:50 (v/v) water/methanol (H_2O/MeOH) for denaturing conditions. Low-concentration Tuning Mix calibration standard (TuneMix, G24221A) was purchased from Agilent Technologies (Santa Clara, CA). Details on the Tuning Mix structures is described elsewhere.[33]

4.2. TIMS-MS Experiments. Ion mobility experiments were performed on a custom-built nano-ESI-TIMS coupled to an Impact Q-TOF mass spectrometer (Bruker, Billerica, MA).[31,32] The TIMS unit is run by custom software in LabView (National Instruments) synchronized with the MS platform controls.[31] Sample aliquots (10 μL) were loaded in a pulled-tip capillary and sprayed at 1200 V. Details regarding the TIMS operation and specifics compared to traditional IMS can be found elsewhere.[31,32] Briefly, the ion mobility separation in a TIMS device is based on holding the ions stationary using an electric field (E) against a moving buffer gas.[50] The TIMS separation depends on the gas flow velocity (v_g), elution voltage ($V_{elution}$), ramp time (t_{ramp}), and base voltage (V_{out}).[32,50] The reduced mobility, K_0, is defined by

$$K_0 = \frac{v_g}{E} \cong \frac{A}{(V_{elution} - V_{out})} \quad (1)$$

The constant A can be determined using calibration standards (Tuning Mix) of known reduced mobilities (K_0 of 1.013, 0.835, and 0.740 $cm^2/(V\ s)$ for respective m/z 622, 922, and 1222).[33] In the TIMS operation, multiple isomers/conformers are trapped simultaneously at different E values resulting from a voltage gradient applied across the IMS tunnel region. After thermalization, isomers/conformers are eluted by decreasing the electric field in stepwise decrements. Each isomer/conformer eluting from the TIMS cell can be described by a characteristic voltage ($V_{elution}$). In a TIMS device, the total analysis time (t_T) can be described as

$$t_T = t_{trap} + \left(\frac{V_{elution}}{V_{ramp}}\right) t_{ramp} + t_{of} \quad (2)$$

where t_{trap} is the thermalization/trapping time, t_{of} is the time after the ion mobility separation, and V_{ramp} and t_{ramp} are the voltage range and time required to vary the electric field, respectively. The elution voltage can be experimentally determined by varying the ramp time for a constant ramp voltage. A linear dependence of t_T with t_{ramp} for all the investigated m/z was obtained as describe elsewhere.[33] From the slope and the intercept of this graph, the mobility values can be determined using the calibration constant A determined with the Tuning Mix component. The measured mobilities were converted into collision cross sections (CCS, Å^2) using the Mason–Schamp equation

$$\Omega = \frac{(18\pi)^{1/2}}{16} \frac{q}{(k_B T)^{1/2}} \left(\frac{1}{m} + \frac{1}{M}\right)^{1/2} \frac{1}{N} \times \frac{1}{K} \quad (3)$$

where q is the ion charge, k_B is the Boltzmann constant, N is the gas number density, m is the ion mass, and M is the gas molecule mass.[50,3] The TIMS separation was carried out using nitrogen (N_2) at ambient temperature (T) with v_g set by the pressure difference between the funnel entrance (P_1 = 2.6 mbar) and exit (P_2 = 1.1 mbar, Figure S7). An radio frequency voltage of 200 V_{pp} at 880 kHz was applied to all the electrodes. Collision-induced activation experiments were performed before the TIMS-MS by increasing the voltage between the capillary outlet (V_{cap}: 40–180 V), deflector plate (V_{def}: 60–200 V), and funnel entrance (V_{fun}: 0–140 V) in 10 V steps.

■ ASSOCIATED CONTENT

Supporting Information

The Supporting Information is available free of charge on the ACS Publications website at DOI: 10.1021/acsomega.8b00375.

Amino acid sequence of the GHRH (1–44) and GHRH (1–29), ion mobility profiles of the observed charge states of the GHRH analogues as a function of the activation energy, ion mobility profiles of the individual charge states of the GHRH analogues, correlation maps of the structural motifs of the GHRH analogues in a denaturing molecular environment, chemical structure of pentafluoro-phenylalanine (Fpa_5), *N*-methyl-tyrosine (*N*-Me-Tyr), and parachloro-phenylalanine (Cpa), scheme of the TIMS cell and tables of the measured CCS for all the GHRH analogue ions (PDF)

■ AUTHOR INFORMATION

Corresponding Author

*E-mail: fernandf@fiu.edu.

ORCID

Francisco Fernandez-Lima: 0000-0002-1283-4390

Author Contributions

The manuscript was written through contributions of all the authors. All the authors have given approval to the final version of the manuscript.

Notes

The authors declare no competing financial interest.

■ ACKNOWLEDGMENTS

The authors acknowledge the financial support from the National Science Foundation Division of Chemistry, under CAREER award CHE-1654274, with co-funding from the Division of Molecular and Cellular Biosciences to F.F.-L.

■ REFERENCES

(1) Schally, A. V.; Varga, J. L.; Engel, J. B. Antagonists of growth-hormone-releasing hormone: an emerging new therapy for cancer. *Nat. Clin. Pract. Endocrinol. Metab.* **2008**, *4*, 33–43.

(2) Rivier, J.; Spiess, J.; Thorner, M.; Vale, W. Characterization of a growth hormone-releasing factor from a human pancreatic islet tumour. *Nature* **1982**, *300*, 276–278.

(3) Ling, N.; Esch, F.; Bohlen, P.; Brazeau, P.; Wehrenberg, W. B.; Guillemin, R. Isolation, primary structure, and synthesis of human hypothalamic somatocrinin: growth hormone-releasing factor. *Proc. Natl. Acad. Sci. U.S.A.* **1984**, *81*, 4302–4306.

(4) Vance, M. L. Growth-hormone-releasing hormone. *Clin. Chem.* **1990**, *36*, 415–420.

(5) Havt, A.; Schally, A. V.; Halmos, G.; Varga, J. L.; Toller, G. L.; Horvath, J. E.; Szepeshazi, K.; Koster, F.; Kovitz, K.; Groot, K.; Zarandi, M.; Kanashiro, C. A. The expression of the pituitary growth hormone-releasing hormone receptor and its splice variants in normal and neoplastic human tissues. *Proc. Natl. Acad. Sci. U.S.A.* **2005**, *102*, 17424–17429.

(6) Guarcello, V.; Weigent, D. A.; Blalock, J. E. Growth hormone releasing hormone receptors on thymocytes and splenocytes from rats. *Cell. Immunol.* **1991**, *136*, 291–302.

(7) Khorram, O.; Yeung, M.; Vu, L.; Yen, S. S. Effects of [norleucine27]growth hormone-releasing hormone (GHRH) (1-

DOI: 10.1021/acsomega.8b00375
ACS Omega 2018, 3, 7432–7440

29)-NH2 administration on the immune system of aging men and women. *J. Clin. Endocrinol. Metab.* **1997**, *82*, 3590−3596.
(8) Schally, A. V. New approaches to the therapy of various tumors based on peptide analogues. *Horm. Metab. Res.* **2008**, *40*, 315−322.
(9) Gallego, R.; Pintos, E.; Garcia-Caballero, T.; Raghay, K.; Boulanger, L.; Beiras, A.; Gaudreau, P.; Morel, G. Cellular distribution of growth hormone-releasing hormone receptor in human reproductive system and breast and prostate cancers. *Histol. Histopathol.* **2005**, *20*, 697−706.
(10) Barabutis, N.; Schally, A. V. Growth hormone-releasing hormone: extrapituitary effects in physiology and pathology. *Cell Cycle* **2010**, *9*, 4110−4116.
(11) Chopin, L. K.; Herington, A. C. A potential autocrine pathway for growth hormone releasing hormone (GHRH) and its receptor in human prostate cancer cell lines. *Prostate* **2001**, *49*, 116−121.
(12) Boulanger, L.; Lazure, C.; Lefrancois, L.; Gaudreau, P. Proteolytic degradation of rat growth hormone-releasing factor(1−29) amide in rat pituitary and hypothalamus. *Brain Res.* **1993**, *616*, 39−47.
(13) Schally, A. V.; Varga, J. Antagonists of Growth Hormone-Releasing Hormone in Oncology. *Comb. Chem. High Throughput Screening* **2006**, *9*, 163−170.
(14) Letsch, M.; Schally, A. V.; Busto, R.; Bajo, A. M.; Varga, J. L. Growth hormone-releasing hormone (GHRH) antagonists inhibit the proliferation of androgen-dependent and -independent prostate cancers. *Proc. Natl. Acad. Sci. U.S.A.* **2003**, *100*, 1250−1255.
(15) Heinrich, E.; Schally, A. V.; Buchholz, S.; Rick, F. G.; Halmos, G.; Mile, M.; Groot, K.; Hohla, F.; Zarandi, M.; Varga, J. L. Dose-dependent growth inhibition in vivo of PC-3 prostate cancer with a reduction in tumoral growth factors after therapy with GHRH antagonist MZ-J-7-138. *Prostate* **2008**, *68*, 1763−1772.
(16) Stangelberger, A.; Schally, A. V.; Varga, J. L.; Zarandi, M.; Szepeshazi, K.; Armatis, P.; Halmos, G. Inhibitory effect of antagonists of bombesin and growth hormone-releasing hormone on orthotopic and intraosseous growth and invasiveness of PC-3 human prostate cancer in nude mice. *Clin. Cancer Res.* **2005**, *11*, 49−57.
(17) Papadia, A.; Schally, A. V.; Halmos, G.; Varga, J. L.; Seitz, S.; Buchholz, S.; Rick, F.; Zarandi, M.; Bellyei, S.; Treszl, A.; Szalontay, L.; Lucci, J. A. Growth hormone-releasing hormone antagonists inhibit growth of human ovarian cancer. *Horm. Metab. Res.* **2011**, *43*, 816−820.
(18) Cai, R.; Schally, A. V.; Cui, T.; Szalontay, L.; Halmos, G.; Sha, W.; Kovacs, M.; Jaszberenyi, M.; He, J.; Rick, F. G.; Popovics, P.; Kanashiro-Takeuchi, R.; Hare, J. M.; Block, N. L.; Zarandi, M. Synthesis of new potent agonistic analogues of growth hormone-releasing hormone (GHRH) and evaluation of their endocrine and cardiac activities. *Peptides* **2014**, *52*, 104−112.
(19) Ludwig, B.; Ziegler, C. G.; Schally, A. V.; Richter, C.; Steffen, A.; Jabs, N.; Funk, R. H.; Brendel, M. D.; Block, N. L.; Ehrhart-Bornstein, M.; Bornstein, S. R. Agonist of growth hormone-releasing hormone as a potential effector for survival and proliferation of pancreatic islets. *Proc. Natl. Acad. Sci. U.S.A.* **2010**, *107*, 12623−12628.
(20) Schubert, U.; Schmid, J.; Lehmann, S.; Zhang, X. Y.; Morawietz, H.; Block, N. L.; Kanczkowski, W.; Schally, A. V.; Bornstein, S. R.; Ludwig, B. Transplantation of pancreatic islets to adrenal gland is promoted by agonists of growth-hormone-releasing hormone. *Proc. Natl. Acad. Sci. U.S.A.* **2013**, *110*, 2288−2293.
(21) Kanashiro-Takeuchi, R. M.; Tziomalos, K.; Takeuchi, L. M.; Treuer, A. V.; Lamirault, G.; Dulce, R.; Hurtado, M.; Song, Y.; Block, N. L.; Rick, F.; Klukovits, A.; Hu, Q.; Varga, J. L.; Schally, A. V.; Hare, J. M. Cardioprotective effects of growth hormone-releasing hormone agonist after myocardial infarction. *Proc. Natl. Acad. Sci. U.S.A.* **2010**, *107*, 2604−2609.
(22) Florea, V.; Majid, S. S.; Kanashiro-Takeuchi, R. M.; Cai, R. Z.; Block, N. L.; Schally, A. V.; Hare, J. M.; Rodrigues, C. O. Agonists of growth hormone-releasing hormone stimulate self-renewal of cardiac stem cells and promote their survival. *Proc. Natl. Acad. Sci. U.S.A.* **2014**, *111*, 17260−17265.
(23) Dioufa, N.; Schally, A. V.; Chatzistamou, I.; Moustou, E.; Block, N. L.; Owens, G. K.; Papavassiliou, A. G.; Kiaris, H. Acceleration of wound healing by growth hormone-releasing hormone and its agonists. *Proc. Natl. Acad. Sci. U.S.A.* **2010**, *107*, 18611−18615.
(24) Pelletier, J. N.; Lortie, R. Sequence-activity relationships guide directed evolution. *Nat. Biotechnol.* **2007**, *25*, 297−298.
(25) Berland, M.; Offmann, B.; Andre, I.; Remaud-Simeon, M.; Charton, P. A web-based tool for rational screening of mutants libraries using ProSAR. *Protein Eng., Des. Sel.* **2014**, *27*, 375−381.
(26) Fenn, J. B.; Mann, M.; Meng, C.; Wong, S.; Whitehouse, C. Electrospray ionization for mass spectrometry of large biomolecules. *Science* **1989**, *246*, 64−71.
(27) Pierson, N. A.; Chen, L.; Valentine, S. J.; Russell, D. H.; Clemmer, D. E. Number of solution states of bradykinin from ion mobility and mass spectrometry measurements. *J. Am. Chem. Soc.* **2011**, *133*, 13810−13813.
(28) Zhong, Y.; Hyung, S. J.; Ruotolo, B. T. Ion mobility-mass spectrometry for structural proteomics. *Expert Rev. Proteomics* **2012**, *9*, 47−58.
(29) Beveridge, R.; Chappuis, Q.; Macphee, C.; Barran, P. Mass spectrometry methods for intrinsically disordered proteins. *Analyst* **2013**, *138*, 32−42.
(30) Schenk, E. R.; Ridgeway, M. E.; Park, M. A.; Leng, F.; Fernandez-Lima, F. Isomerization Kinetics of AT Hook Decapeptide Solution Structures. *Anal. Chem.* **2014**, *86*, 1210−1214.
(31) Fernandez-Lima, F. A.; Kaplan, D. A.; Park, M. A. Note: Integration of trapped ion mobility spectrometry with mass spectrometry. *Rev. Sci. Instrum.* **2011**, *82*, No. 126106.
(32) Fernandez-Lima, F.; Kaplan, D. A.; Suetering, J.; Park, M. A. Gas-phase separation using a Trapped Ion Mobility Spectrometer. *Int. J. Ion Mobility Spectrom.* **2011**, *14*, 93−98.
(33) Hernandez, D. R.; Debord, J. D.; Ridgeway, M. E.; Kaplan, D. A.; Park, M. A.; Fernandez-Lima, F. Ion dynamics in a trapped ion mobility spectrometer. *Analyst* **2014**, *139*, 1913−1921.
(34) Adams, K. J.; Montero, D.; Aga, D.; Fernandez-Lima, F. Isomer Separation of Polybrominated Diphenyl Ether Metabolites using nanoESI-TIMS-MS. *Int. J. Ion Mobility Spectrom.* **2016**, *19*, 69−76.
(35) Li, J.; Taraszka, J. A.; Counterman, A. E.; Clemmer, D. E. Influence of solvent composition and capillary temperature on the conformations of electrosprayed ions: unfolding of compact ubiquitin conformers from pseudonative and denatured solutions. *Int. J. Mass Spectrom.* **1999**, *185*−*187*, 37−47.
(36) Wang, F.; Freitas, M. A.; Marshall, A. G.; Sykes, B. D. Gas-phase memory of solution-phase protein conformation: H/D exchange and Fourier transform ion cyclotron resonance mass spectrometry of the N-terminal domain of cardiac troponin C. *Int. J. Mass Spectrom.* **1999**, *192*, 319−325.
(37) Schenk, E. R.; Almeida, R.; Miksovska, J.; Ridgeway, M. E.; Park, M. A.; Fernandez-Lima, F. Kinetic Intermediates of Holo- and Apo-Myoglobin Studied Using HDX-TIMS-MS and Molecular Dynamic Simulations. *J. Am. Soc. Mass Spectrom.* **2015**, *26*, 555−563.
(38) Molano-Arevalo, J. C.; Hernandez, D. R.; Gonzalez, W. G.; Miksovska, J.; Ridgeway, M. E.; Park, M. A.; Fernandez-Lima, F. Flavin adenine dinucleotide structural motifs: from solution to gas phase. *Anal. Chem.* **2014**, *86*, 10223−10230.
(39) Garabedian, A.; Butcher, D.; Lippens, J. L.; Miksovska, J.; Chapagain, P. P.; Fabris, D.; Ridgeway, M. E.; Park, M. A.; Fernandez-Lima, F. Structures of the kinetically trapped i-motif DNA intermediates. *Phys. Chem. Chem. Phys.* **2016**, *18*, 26691−26702.
(40) Molano-Arevalo, J. C.; Jeanne Dit Fouque, K.; Pham, K.; Miksovska, J.; Ridgeway, M. E.; Park, M. A.; Fernandez-Lima, F. Characterization of Intramolecular Interactions of Cytochrome c Using Hydrogen-Deuterium Exchange-Trapped Ion Mobility Spectrometry-Mass Spectrometry and Molecular Dynamics. *Anal. Chem.* **2017**, *89*, 8757−8765.
(41) Molano-Arevalo, J. C.; Gonzalez, W.; Jeanne Dit Fouque, K.; Miksovska, J.; Maitre, P.; Fernandez-Lima, F. Insights from ion

DOI: 10.1021/acsomega.8b00375
ACS Omega 2018, 3, 7432−7440

mobility-mass spectrometry, infrared spectroscopy, and molecular dynamics simulations on nicotinamide adenine dinucleotide structural dynamics: NAD(+) vs. NADH. *Phys. Chem. Chem. Phys.* **2018**, *20*, 7043−7052.
(42) Zhong, Y.; Han, L.; Ruotolo, B. T. Collisional and Coulombic unfolding of gas-phase proteins: high correlation to their domain structures in solution. *Angew. Chem., Int. Ed.* **2014**, *53*, 9209−9212.
(43) Shi, H.; Atlasevich, N.; Merenbloom, S. I.; Clemmer, D. E. Solution dependence of the collisional activation of ubiquitin [M + 7H](7+) ions. *J. Am. Soc. Mass Spectrom.* **2014**, *25*, 2000−2008.
(44) Hamamoto, K.; Kida, Y.; Zhang, Y.; Shimizu, T.; Kuwano, K. Antimicrobial Activity and Stability to Proteolysis of Small Linear Cationic Peptides with D-Amino Acid Substitutions. *Microbiol. Immunol.* **2002**, *46*, 741−749.
(45) Tugyi, R.; Uray, K.; Ivan, D.; Fellinger, E.; Perkins, A.; Hudecz, F. Partial D-amino acid substitution: Improved enzymatic stability and preserved Ab recognition of a MUC2 epitope peptide. *Proc. Natl. Acad. Sci. U.S.A.* **2005**, *102*, 413−418.
(46) Jeanne Dit Fouque, K.; Garabedian, A.; Porter, J.; Baird, M.; Pang, X.; Williams, T. D.; Li, L.; Shvartsburg, A.; Fernandez-Lima, F. Fast and Effective Ion Mobility-Mass Spectrometry Separation of d-Amino-Acid-Containing Peptides. *Anal. Chem.* **2017**, *89*, 11787−11794.
(47) Zarandi, M.; Cai, R.; Kovacs, M.; Popovics, P.; Szalontay, L.; Cui, T.; Sha, W.; Jaszberenyi, M.; Varga, J.; Zhang, X.; Block, N. L.; Rick, F. G.; Halmos, G.; Schally, A. V. Synthesis and structure-activity studies on novel analogs of human growth hormone releasing hormone (GHRH) with enhanced inhibitory activities on tumor growth. *Peptides* **2017**, *89*, 60−70.
(48) Fahrenholtz, C. D.; Rick, F. G.; Garcia, M. I.; Zarandi, M.; Cai, R. Z.; Block, N. L.; Schally, A. V.; Burnstein, K. L. Preclinical efficacy of growth hormone-releasing hormone antagonists for androgen-dependent and castration-resistant human prostate cancer. *Proc. Natl. Acad. Sci. U.S.A.* **2014**, *111*, 1084−1089.
(49) Zarandi, M.; Horvath, J. E.; Halmos, G.; Pinski, J.; Nagy, A.; Groot, K.; Rekasi, Z.; Schally, A. V. Synthesis and biological activities of highly potent antagonists of growth hormone-releasing hormone. *Proc. Natl. Acad. Sci. U.S.A.* **1994**, *91*, 12298−12302.
(50) McDaniel, E. W.; Mason, E. A. *Mobility and Diffusion of Ions in Gases*; John Wiley and Sons, Inc.: New York, 1973; p 381.

DOI: 10.1021/acsomega.8b00375
ACS Omega 2018, 3, 7432−7440